Transonic Laminar Viscous-Inviscid Interaction over Airfoils

Tsze C. Tai*
Naval Ship Research and Development Center, Bethesda, Md.

A theoretical model consisting of an inviscid external flow and a viscous boundary-layer flow is formulated for the subject problem. Procedures developed independently, for these two separate flows are combined to enable an analysis of the viscous-inviscid interaction problem at transonic speeds. Both attached and separated boundary layers are considered for either weak or strong interactions. The systems of resulting ordinary differential equations for both flows are coupled by the streamline angle of the inviscid flow at the edge of the boundary layer and are integrated simultaneously for strong interactions. The weak interaction is accounted for by simply correcting the airfoil surface with the boundary-layer displacement thickness. Theoretical results are in good agreement with recent laminar experimental data. It is found that for supercritical flows, a strong interaction usually occurs regardless of whether the laminar boundary layer is attached or separated. The viscous-inviscid interaction process terminates the embedded supersonic flow earlier than does the inviscid shock.

Nomenclature

a = speed of sound; also profile parameter
C = $1+2/[(\gamma-1)M_\infty^2]$
C_p = pressure coefficient
c = chord length of an airfoil
H = θ_i/δ_i^*, the shape factor
J,Q,R,Z = velocity profile quantities
K = $1/(\gamma M_\infty^2)$
M = Mach number
N = number of effective regions
P = static pressure normalized by its freestream value
Re = Reynolds number
S = entropy
s,n = orthogonal curvilinear coordinates measured along and normal to the airfoil surface, normalized by the chord length
U,V = velocity components in Cartesian coordinates, normalized by the freestream velocity
u,v = velocity components along and normal to the airfoil surface, normalized by the freestream velocity
V_∞ = freestream velocity
x,y = Cartesian coordinates normalized by the chord length
α = angle of attack
β = oblique shock angle
γ = specific heat ratio
δ = boundary-layer thickness
δ^* = boundary-layer displacement thickness normalized by the chord length
Θ = induced streamline inclination at the edge of boundary layer with respect to local surface
θ = surface inclination with respect to the direction of freestream velocity
θ_i = transformed boundary-layer momentum thickness
μ = viscosity
ν = kinematic viscosity
ρ = gas density normalized by its freestream value

Subscripts

e = edge of boundary layer
i = transformed incompressible plane
j = jth field strip boundary
0 = initial condition
$1,2$ = conditions before and after shock wave
∞ = freestream condition

Introduction

SEVERAL methods are available for determining the inviscid transonic flow about airfoils. The strength and the location of the embedded shock wave predicted by such methods generally differ from experimental measurements because of the viscous effect near the surface of the airfoil.[1-3] If the shock wave is strong enough to cause flow separation, the viscous layer thickens rapidly. In such cases, the surface flow properties cannot be specified in advance, as in the usual formulation of boundary-layer theory, but are determined by interaction of the outer inviscid flow and the inner viscous flow near the surface. This has been referred to as the transonic viscous-inviscid interaction problem.

The phenomenon of the transonic viscous-inviscid interaction was first investigated experimentally by Liepmann[4] and Ackeret et al.[5] Previous theoretical analyses on viscous-inviscid interactions have been concerned primarily with supersonic external flows. Those by Lighthill,[6] Lees and Reeves,[7] and Klineberg and Lees[8] are typical examples.

In contrast to supersonic free interaction, the problem of viscous-inviscid interaction in the transonic region is complicated by the fact that the inviscid flowfield is governed by mixed elliptic and hyperbolic partial differential equations for a compressible fluid flow. Because the major portion of the flowfield is of the elliptic type, the velocity at the edge of the boundary-layer at any location depends on the complete displacement thickness distribution. At the same time, the solution must satisfy the constraints characterized by the inviscid supercritical flows—the regularity condition at sonic points. The complete solution, therefore, involves tedious iterative procedures. Some advances in the area of laminar viscous-inviscid interactions at transonic speeds were recently made by Klineberg and Steger[9] and Brilliant and Adamson.[10] The former paper treats the interaction by using a boundary-

Presented as Paper 74-600 at the AIAA 7th Fluid and Plasma Dynamics Conference, Palo Alto, California, June 17-19, 1974; submitted August 5, 1974; revision received February 20, 1975. This research was sponsored by the Naval Air Systems Command (AIR-320). The author wishes to thank H.R. Chaplin, Jr., for his interest and support and S. de los Santos for his valuable suggestions and encouragement. Thanks are also due to J.M. Klineberg of NASA for his numerous helpful discussions.

Index categories: Subsonic and Transonic Flow; Jets, Wakes, and Viscid-Inviscid Flow Interactions.

*Research Aerospace Engineer, Aviation and Surface Effects Department. Member AIAA.

layer integral approach, combined with a finite difference-relaxation method for the small disturbance equations of the external flow. Inviscid and viscous flows are treated separately even for strong interactions. The latter uses the method of matched asymptotic expansion for an incident shock interacting with an unseparated laminar boundary layer in transonic flow.

In the present paper, the transonic inviscid solution by the method of integral relations[11,12] is coupled with the integral method, developed by Lees and Reeves[7] and refined by Klineberg and Lees[8] for compressible attached and separated laminar boundary layers. The transonic inviscid solution replaces the simple Prandtl-Meyer relations originally used for supersonic free interactions.

Theoretical Considerations

Description of Transonic Viscous-Inviscid Interaction

The schematic of the transonic viscous-inviscid interaction over an airfoil surface is represented in Fig. 1. The embedded supersonic region of a supercritical flow has to be terminated by a shock wave to bring the downstream flow back to the subsonic state, and the shock foot is smeared into a series of compression waves as a result of viscous-inviscid interactions. The presence of an adverse pressure gradient due to the compression before the shock usually causes the boundary layer to separate from the surface for either laminar or turbulent boundary layers. However, the flow behavior near the shock differs considerably, depending on whether the boundary layer is laminar or turbulent ahead of the point where it meets the shock.[13] The pressure rises more rapidly for turbulent than for laminar layers,[1,13] while the displacement thickness of the boundary layer increases considerably through the shock, more so for laminar than for turbulent layers.[5] Reynolds number has a strong effect on the interaction in the case of laminar boundary layers but almost no effect for turbulent flows.[1,5] In any event, the basic features of boundary-layer thickening and pressure rising are common for both layers.

Beyond the separation point, the boundary-layer flow is divided into two regions by the dividing streamline.[7,14,15] The flow above this streamline includes all the fluid contained in the boundary layer just upstream of separation. Below this streamline, the flow yields a separated pattern with reversed profile near the wall. Two kinds of separated-flow pattern have been observed by Pearcey et al. for turbulent boundary layers.[16] One deals with a local separation bubble caused by the shock; the other is involved with rear separation and depends on the magnitude of the pressure gradient approaching the trailing edge and on the upstream history of the boundary layer.

The pressure rises continuously in the subsonic portion although its gradient decreases steadily after the toe of the shock.[16] This feature differs from that of a supersonic free interaction in which the incident shock is reflected as an expansion fan which turns the flow toward the surface and thus enables the reattachment of the boundary layer.[7] In the transonic case, however, the shock is an embedded one which serves as part of the compression process of the flow over the rear of the airfoil; whereas, the boundary layer, especially the laminar one, does not have sufficient energy for reattachment against continuous adverse presure gradients and, therefore, remains separated all the way toward the trailing edge.

Strong vs Weak Interactions in Laminar Flows

In analysis of viscous transonic flows, it is necessary for the analytical model of the viscous system to have the capability of allowing communication of positive pressure disturbance from the embedded shock wave upstream through the subsonic portion of the boundary layer. The usual formulation of the boundary-layer theory in which the boundary-layer properties are dictated by the inviscid solution through the specified pressure distribution does not provide such a capability. The positive pressure disturbance which propagates upstream from the shock wave exerts no influence on the boundary-layer behavior. The solution experiences a discontinuity at the shock as dictated by the inviscid pressure jump, rather than a gradual increase as experimentally observed.

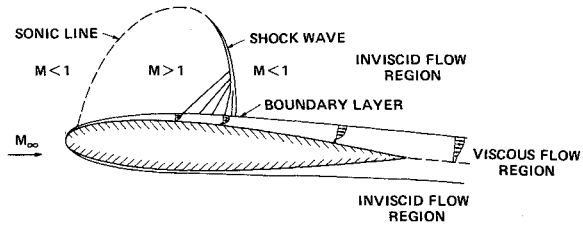

Fig. 1 Transonic viscous-inviscid interaction over airfoils.

Such a discrepancy may be removed by solving the outer inviscid and inner boundary-layer flows simultaneously. The two flows are coupled by a common variable with the surface pressure being calcualted by the viscous equations to directly account for the propagation of positive pressure disturbance upstream through the viscous layer. The communication of the pressure disturbance through the viscous layer becomes possible in the sense that the flow inside the viscous layer is subcritical and that the laminar boundary layer is no longer dictated by the inviscid pressures. The viscous system is linked to the inviscid system through a common variable by which the change of flow properties of the outer flow may be transmitted to the inner flow, or vice versa. The new system model is referred to as the strong interaction formulation; the usual boundary-layer system, as the weak interaction.

The strong interaction formulation may be applied to attached, as well as separated, laminar boundary layers. When applied to attached flows, the boundary layer usually separates in a short distance. If the same flow were to be treated by the weak interaction system, numerical experiments indicate that the boundary layer would remain attached until shock jump was encountered. This gives further indication that the strong interaction system is more suitable in simulating the shock wave/boundary-layer interaction process than is the usual boundary-layer correction. On the other hand, the use of weak interaction formulation is preferred in the forward portion of the airfoil where the viscous-inviscid interaction is presumably weak.

Inviscid Flow

Governing Equations

The partial differential equations that govern a steady, inviscid flow can be written in a Cartesian coordinate system as

Continuity:

$$\partial(\rho U)/\partial x+\partial(\rho V)/\partial y=0 \tag{1}$$

x-Momentum:

$$\partial/\partial x(KP+\rho U^2)+\partial/\partial y(\rho UV)=0 \tag{2}$$

y-Momentum:

$$\partial/\partial x(\rho UV)+\partial/\partial y(KP+\rho V^2)=0 \tag{3}$$

State:

$$P=\rho^{\gamma}\exp(P_2/\rho_2{}^{\gamma}) \tag{4}$$

The boundary conditions are as follows: at the edge of the

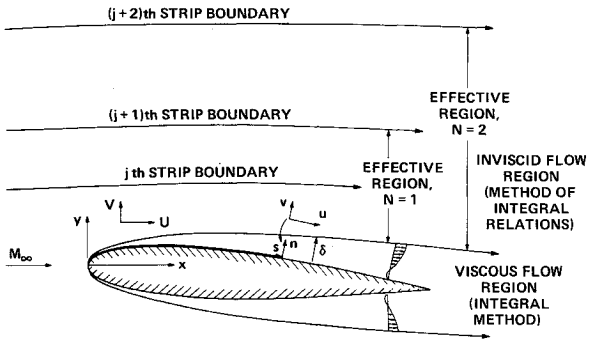

Fig. 2 Coordinate systems and flow regions.

boundary layer, the vertical velocity is coupled to that of the viscous system, i.e.,

$$V_e = M_e a_e \sin(\Theta + \theta) \tag{5a}$$

at infinity, the flow is undisturbed, i.e.,

$$P = \rho = U = 1; \quad V = 0 \tag{5b}$$

Method of Integral Relations

The inviscid flowfield is treated as a series of different effective regions; a two-strip approximation is incorporated in each region. The solution of the outer region provides the boundary condition for the next inner region, and so on.[11,12] Therefore, one needs only to determine flow properties along two-strip boundaries in each region, the base boundary and the field boundary; see Fig. 2. The merit of the new strip arrangement is that it allows the use of a large number of strips without requiring the higher-order polynomials which usually cause numerical difficulties in actual computation. To apply the scheme to the present problem, the base boundary is set at the edge of the boundary layer. The field strip boundaries are set up exactly the same way as in the inviscid cases.[11,12]

Inviscid Ordinary System

The ordinary differential equations for the inviscid external flow reduced by means of the N-2-strip integration scheme associated with the method of integral relations are

$$dU_e/dx = F_e \tag{6}$$

$$dV_e/dx = G_e \tag{7}$$

$$\rho_e = \left[\frac{C - U_e^2 - V_e^2}{C-1}\right]^{1/\gamma-1} \tag{8}$$

$$P_e = \rho_e^{\gamma} \tag{9}$$

$$dU_j/dx = F_j \tag{10}$$

$$dV_j/dx = G_j \tag{11}$$

$$\rho_j = \left[\frac{(C-1)(P_{t_2}/\rho_{t_2})_j - U_j^2 - V_j^2}{(C-1)(P_2/\rho_2^{\gamma})_j}\right]^{1/(\gamma-1)} \tag{12}$$

$$P_j = \rho_j^{\gamma} \exp(P_2/\rho_2^{\gamma})_j \tag{13}$$

where F_e, G_e, F_j, and G_j have been given elsewhere.[17] The subscript e denotes the condition at the edge of the boundary layer; the index j, the condition at the jth field-strip boundary; j varies from 1 to N, where N is the number of effective regions; see Fig. 2. The total number of strips is $\bar{N} = N+1$. Note that Eqs. (12) and (13) allow entropy change across the shock wave which retains a finite strength in the external flowfield.

Viscous Flow

Governing Equations

In view of the thick viscous layer involved in the separated-flow region, it would be appropriate to integrate the full set of Navier-Stokes equations in the present problem. However, boundary-layer equations are still adequate for describing the essential physical features of the viscous flow. The application of the boundary-layer method in the separated region has been proved a posteriori for the supersonic free interactions.[7,8] In the present analysis, the Reynolds number of the flow is kept sufficiently large to further assure the validity of the thin boundary-layer approximation.

The governing equations for a compressible laminar boundary-layer flow in coordinates parallel and normal to the surface are

Continuity:

$$\frac{\partial(\rho u)}{\partial s} + \frac{\partial(\rho v)}{\partial n} = 0 \tag{14}$$

s-Momentum:

$$\rho u \frac{\partial u}{\partial s} + \rho v \frac{\partial u}{\partial n} = -K \frac{dP}{ds} + \frac{1}{\rho_\infty V_\infty c} \frac{\partial}{\partial n}\left[\mu \frac{\partial u}{\partial n}\right] \tag{15}$$

The boundary conditions are as follows: at the surface, $u = v = 0$; at the edge of the boundary layer, $u = u_e(s)$ for weak interaction, and $u^2 + v^2 = V_e^2 / \sin^2(\Theta + \theta)$ for strong interaction. It is noticed that V_e is obtained from the inviscid solution. The coupling of the viscous and inviscid flows is discussed in detail later.

Integral Method

An integral method is employed in the viscous region for both attached and separated laminar boundary layers. Following the procedure of Klineberg and Lees,[8] the governing equations for the viscous flow, Eqs. (14) and (15), are transformed into an equivalent incompressible form by means of the Stewartson transformation.[18] The velocity profile based on an incompressible similarity solution can therefore be used in the integral approach. The resulting partial differential equations in a transformed incompressible plane, along with the equation for the rate of change of mechanical energy, i.e., the moment of momentum, are then integrated across the boundary-layer from $n = 0$ to $n = \delta$. In performing the integration, the parameter a is employed to denote the velocity profile for both attached and separated boundary layers. Profile quantities are then defined as functions of a.[8] For attached boundary layers, the parameter a possesses a physical meaning in that it is proportional to the shearing stress at the wall.[19] The separated velocity profiles are analogous to the "lower branch" of the similarity solution found by Stewartson.[20]

Viscous Ordinary System for Strong Interactions

The resulting ordinary differential equations are

$$d\delta_i^*/ds = N_1/D \tag{16}$$

$$da/ds = N_2/D \tag{17}$$

$$dM_e/ds = N_3/D \tag{18}$$

where

$$D = \frac{\delta_i^*}{M_e a_e P_e}\left[(Hf - 2HF - F)\frac{dJ}{dH} + J(1 - H + 3F - f)\right] \tag{19}$$

$$N_1=\frac{\delta_i^*}{M_e}\left[\frac{M_\infty}{M_eRe_{\delta_i^*}}\left[Q(f\frac{dJ}{dH}-3J)+R(2H+1-f)\right]+\frac{(1+m_e)\tan\Theta}{m_e(1+m_\infty)}\left[3J-(2H+1)\frac{dJ}{dH}\right]\right] \quad (20)$$

$$N_2=\frac{1}{M_e(dH/da)}\left[\frac{M_\infty}{M_eRe_{\delta_i^*}}\left[JQ(3F-f)+R(Hf-2HF-F)\right]+\frac{(1+m_e)\tan\Theta}{m(1+m_\infty)}J(1-H)\right] \quad (21)$$

$$N_3=\frac{M_\infty}{M_eRe_{\delta_i^*}}\left[Q(J-F(dJ/dH)+R(F-H)\right]+\frac{(1+m_e)\tan\Theta}{m_e(1+m_\infty)}(H\frac{dJ}{dH}-J) \quad (22)$$

$$F=H+(1+m_e)/m_e \quad (23)$$

$$f=(2+\frac{\gamma+1}{\gamma-1}\frac{m_e}{1+m_e})H+\frac{3\gamma-1}{\gamma-1}+\frac{M_e^2-1}{m_e(1+m_e)}Z \quad (24)$$

$$m=(\gamma-1)M^2/2 \quad (25)$$

$$Re_{\delta_i^*}=V_\infty\delta_i^*c/\nu_\infty \quad (26)$$

where variables a, H, J, Q, R, and Z have been defined in Ref. 8. Curve-fitted polynomials, based on the similarity solution of the classical boundary-layer theory, are given in Ref. 8 for attached and separated flows, and in Ref. 21 for wake-reverse and wake-forward flows. They are summarized in Ref. 17.

Reduced Viscous System for Weak Interaction

In case of weak interactions, the static pressure at the edge of the boundary layer is specified by the inviscid solution for which the boundary-layer properties are calculated. The value for dM_e/ds then becomes an input term. The system of equations is reduced to

$$\frac{d\delta_i^*}{ds}=\left[\frac{M_\infty a_eP_e}{M_eRe_{\delta_i^*}}(Q\frac{dJ}{dH}-R)+\frac{\delta_i^*}{M_e}\left[3J-(2H+1)\frac{dJ}{dH}\right]\frac{dM_e}{ds}\right]/(H\frac{dJ}{dH}-J) \quad (27)$$

$$\frac{da}{ds}=\left[\frac{M_\infty a_eP_e}{M_e\delta_i^*Re_{\delta_i^*}}(HR-JQ)+J(1-H)\frac{1}{M_e}\frac{dM_e}{ds}\right]/\left[\frac{dH}{da}H\frac{dJ}{dH}-J)\right] \quad (28)$$

The reduced system of equations has a saddle-type singularity when $J=H(dJ/dH)$. It corresponds to $a=0$, i.e., the location of separation. It is therefore related to the separation-point singularity of the classical boundary-layer theory.

Initial Conditions for Viscous Flow

Because of M_e terms in the denominator of the weak interaction equations, the viscous solution has to start a short distance away from the stagnation point. According to Klineberg and Steger,[9] the flow near the leading edge is locally similar, i.e.

$$dH/ds\cong 0 \quad \text{or} \quad da/ds\cong 0 \quad (29)$$

The derivation procedure is simplified for thin airfoils where the small disturbance approximation is valid. Therefore, we will use small disturbance equations for determining the initial conditions and then evaluate the validity of the approximation for the case of blunt airfoils.

With the small disturbance approximation, the differential equations for the weak interaction [Eqs. (27) and (28)] can be written as[9]

$$\frac{d\delta_i^*}{ds}=\left[\frac{1}{Re_{\delta_i^*}}(Q\frac{dJ}{dH}-R)+\delta_i^*[3J-(2H+1)\frac{dJ}{dH}]\frac{dM_e}{ds}\right]/(H\frac{dJ}{dH}-J) \quad (30)$$

$$\frac{da}{ds}=\left[\frac{1}{\delta_i^*Re_{\delta_i^*}}(HR-JQ)+J(1-H)\frac{dM_e}{ds}\right]/\left[\frac{dH}{da}(H\frac{dJ}{dH}-J)\right] \quad (31)$$

Substituting Eq. (31) into Eq. (30) and integrating with constant profile quantities in accordance with Eq. (29), there results

$$\delta_i^*=\left[\frac{2\nu_\infty}{V_\infty}\frac{R+2HR-3QJ}{J(1-H)}s_o\right]^{1/2} \quad (32)$$

Elimination of δ_i^* between Eqs. (31) and (32) with the aid of Eq. (29) leads to

$$QJ-HR=2(R+2HR-3QJ)s_o(dM_e/ds)_o \quad (33)$$

The value of a at the initial point is obtained by solving Eq. (33) numerically from the known initial arc length s_o and velocity gradient $(dM_e/ds)_o$. The initial value for δ_i^* is then found from Eq. (32).

As mentioned previously, Eqs. (32) and (33) will be good only in case of thin airfoils for which the small disturbance approximation is valid. In fact, the numerical results show that the final values of δ_i^* and a are insensitive to their initial conditions. This is indicated in Figs. 5 and 6 of Ref. 17 where the values of a and δ_i^* are plotted vs x for the case of an NACA 0015 airfoil at $M_\infty=0.729$ and $\alpha=4°$. The independence may be attributed to the fact that the airfoil surface has been updated repeatedly during the solution process; thus, some inaccuracies of the initial conditions may have been absorbed in the iteration process. For these reasons, Eqs. (32) and (33) can also be employed for blunt airfoils.

Coupling of Two Flows

In case of strong interactions, the viscous system is coupled directly to the inviscid system by the induced angle of inviscid streamline at the edge of the boundary layer

$$\Theta=\sin^{-1}\left[\frac{V_{e(\text{inviscid})}}{M_ea_{e(\text{viscous})}}\right]-\theta \quad (34)$$

where V_e is calculated by the inviscid system, while the velocity magnitude M_ea_e is obtained by the viscous system. The variable Θ is a common variable for both inviscid and viscous systems and, therefore, governs the viscous-inviscid interaction process. Since the two flows are coupled by the inviscid streamline angle rather than the streamline itself, mass transfer between the outer inviscid and inner boundary-layer flows is allowed in accordance with the continuity equations by which the variable Θ is introduced in the viscous system.

$$d\delta^*/ds=\tan\Theta+(\delta-\delta^*)\,d/ds[\ln(\rho_eu_e)] \quad (35)$$

The value of Θ, which is determined by the viscous-inviscid

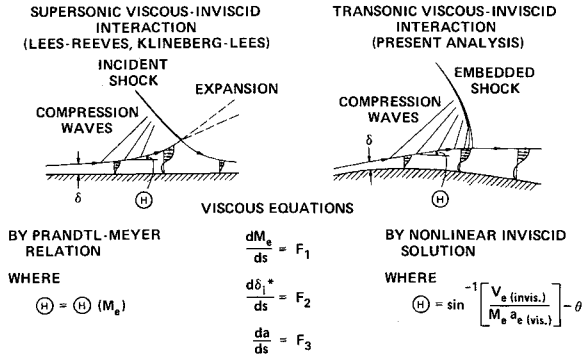

Fig. 3 Analysis of viscous-inviscid interaction.

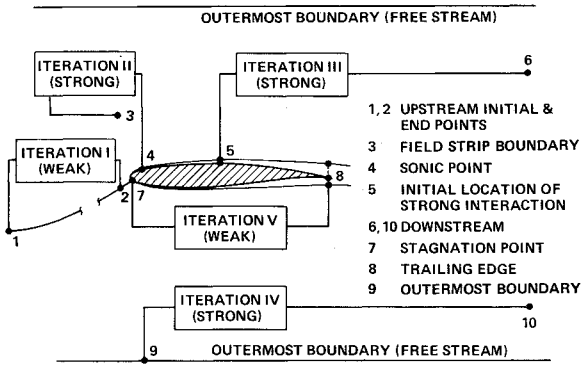

Fig. 4 Iteration procedures for solving the subject two-point boundary value problems.

interaction, has direct bearing on the growth of the boundary layer.

The use of Θ as the interaction parameter is analogous to that in supersonic free-interaction problems[7,8] (see Fig. 3). However, in the present analysis, the transonic inviscid solution replaces the Prandtl-Meyer relations $\Theta = \Theta(M_e)$ as used in supersonic free interactions.[7,8] The present approach also differs from that of Klineberg and Steger[9] in which the V_e values were prescribed rather than calculated. Although the prescribed V_e values were improved successively, the viscous and inviscid flows had to be treated separately even for strong interactions.

$$U_e = (M_e^2 a_e^2 - V_e^2)^{1/2} \tag{36}$$

Therefore, Eq. (6) of the inviscid system, which also gives U_e, becomes redundant.

For weak interactions, the inviscid and viscous flows are linked indirectly. As in a usual procedure, the boundary-layer quantities are calculated based on the specified inviscid pressure distribution, and the inviscid solution is updated based on the surface augmented by the boundary-layer displacement thickness. In so doing, the two flows are connected at the locus of the boundary-layer displacement thickness. The latter serves as a "streamline" through which mass transfer or more importantly, direct communication between the outer inviscid and inner boundary-layer flows is prohibited.

The inviscid equations associated with the weak interaction are the same for the strong interaction, except that here Eq. (6) for U_e must be used, and Eq. (7) for V_e is replaced by the condition at the edge of the boundary layer.

$$V_e = U_e \tan(\Theta + \theta) \tag{37}$$

Numerical Calculations

With the previously described set of ordinary differential equations for both inviscid and viscous flows, the numerical

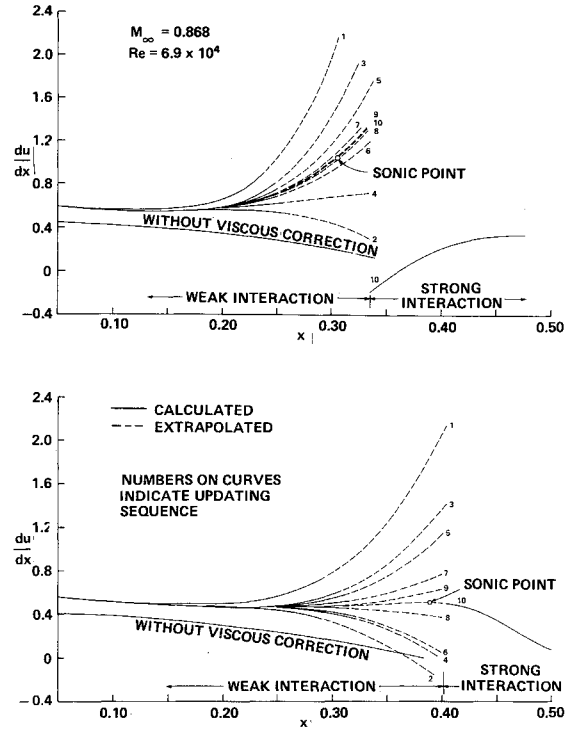

Fig. 5 Determination of initial location of strong interaction region for a 6% circular arc.

integrations were carried out simultaneously for both flows along the longitudinal axis x by using a standard fourth-order Runge-Kutta method. Similar to the inviscid problem,[12] the complete solution procedure consists of five iteration processes which are illustrated in Fig. 4 and are briefly described as follows.

Upstream Integration (Iteration I)

The iteration process here is concerned with the feedback of the geometric and flow properties in the stagnation region to the upstream flow. Since no boundary layer builds up in the upstream, the iteration process is identical to that for a pure inviscid flow.[12]

Treatment of Sonic Point (Iteration II)

The sonic point regularity condition in a supercritical flow is satisfied by an iteration process using the weak interaction equations. The procedure is exactly the same as for the inviscid flow,[12] except that the airfoil surface is augmented by the boundary-layer displacement thickness. The inviscid flow is then recalculated on the basis of the newly augmented surface, and the resulting pressure distribution is used for another round of viscous computation. The procedure is repeated until the updating is converged. If the strong interaction takes place immediately after the sonic point, the present iteration is combined with that for the initial location of the strong interaction region as shown in Fig. 5.

Determination of Initial Location of Strong Interaction Region (Iteration III)

The iteration process for the initial location of the strong interaction region is equivalent to that for the determination of the shock-foot location in a pure inviscid flow,[12] since the shock foot is smeared in the strong interactions, whereas, the upper portion of the shock still retains a finite strength in the external inviscid flow. Unlike the case of pure inviscid flow, here the pressure disturbance caused by the shock can be propagated upstream in the embedded supersonic region through the viscous portion of the flow.

During the iteration process, the strong interaction calculations are initiated at a number of assumed locations. The values of the boundary-layer displacement thickness δ_i^*

and the velocity profile parameter a are kept continuous at these locations. Furthermore, the velocity gradient at the edge of the boundary layer is made continuous by adjusting the inclination of inviscid streamline at the edge of the boundary layer. The integration resumes down to the trailing edge and finally through the downstream region.† The results for each assumed initial location of the strong interaction are then checked to determine whether the downstream boundary condition is satisfied by a bracketing procedure, i.e., the freestream value if bracketed by two integral curves based on two initial locations.[12] If the strong interaction takes place immediately after the sonic point, the iteration process for the forward sonic point is combined with that for the initial location of the strong interaction region as mentioned previously.

Integration for Subcritical Flow (Iteration IV)

The iteration developed here for the integration of subcritical flow is basically similar to that of the inviscid formulation,[12] except that the airfoil surface is repeatedly updated by the boundary-layer displacement thickness in accordance with the weak interaction formulation.

Enforcement of Kutta Condition (Iteration V)

One way of stating the Kutta condition is that the velocity discontinuity at the trailing edge be zero.[22] Since the static pressure is assumed to be constant across the boundary layer, the Kutta condition is satisfied by matching the static pressures at the trailing edge from integrations along both the upper and lower surfaces. The iteration procedure is therefore very much the same as in the inviscid formulation,[12] except that here the viscous-inviscid interactions are accounted for according to the aforementioned procedures.

The above procedures are formulated for flow conditions where the shock wave does not touch the boundary of the strip adjacent to the airfoil. This boundary is usually set between 0.7-0.9 chord length to allow a full development of the local supersonic flow. In fact, the present size of the supersonic pocket covers almost all supercritical flows of practical interests. The physical boundary has even less restraint on the severity of the viscous-inviscid interaction since the latter depends on how favorable the supersonic flow is developed[23] rather than on the size of the embedded supersonic region.

Results and Discussion

Results of calculations at supercritical freestream Mach numbers are presented for both a 6% circular arc and an NACA 0015 airfoil. Flow conditions were chosen to enable comparisons with available experimental data. Since Iterations II-IV were nonnegotiable, they were all carried out accordingly. Iterations I and V converged converged within 2.5%.

The viscous results were calculated in terms of boundary-layer quantities in a transformed incompressible plane. Figure 6 gives the boundary-layer displacement thickness throughout a 6% circular arc airfoil at $M_\infty = 0.868$ and $Re_\infty = 6.9 \times 10^4$. The thickening of the boundary layer in the forward portion follows a similar trend as that found by Schubauer, using the Karman-Polhausen method;[24] however, the present method gives a far more realistic δ distribution pattern in the rear portion.

The corresponding distribution of the boundary-layer shape factor H and the parameter a is presented in Fig. 7. The boundary layer is practically of the Blasius type ($a = 1.857$) in the leading-edge region and varies slightly throughout the forward portion of the airfoil. It remains unseparated through

†The integration in the downstream region is carried out simultaneously for both the upper and lower flowfields with a dividing streamline that separates the shear layers shed from the trailing edge. The geometry of the dividing streamline is determined in such a way that slope vanishes from the trailing edge value asymptotically in the downstream.

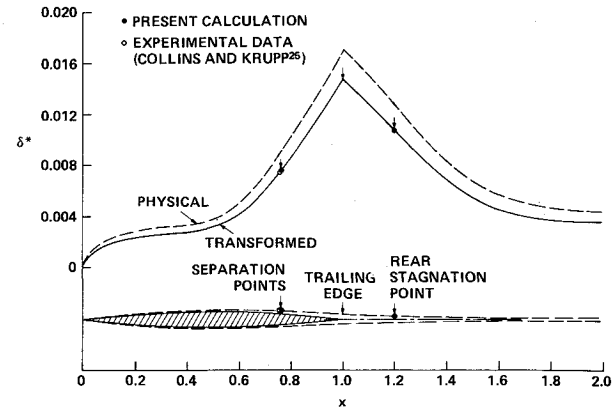

Fig. 6 Boundary-layer displacement thickness for a 6% circular arc at $M_\infty = 0.868$ and $Re_\infty = 6.9 \times 10^4$.

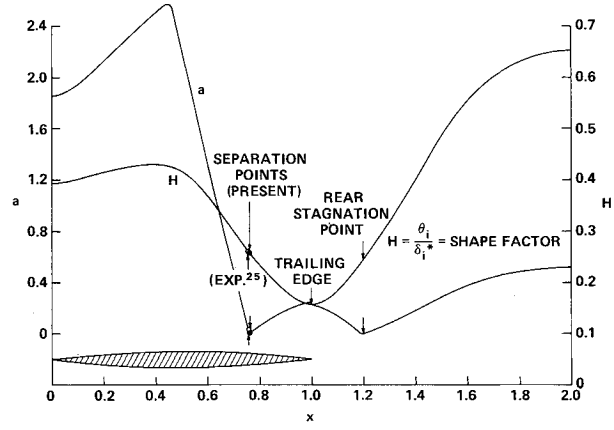

Fig. 7 Velocity profile parameter and shape factor for a 6% circular arc at $M_\infty = 0.868$ and $Re_\infty = 6.9 \times 10^4$.

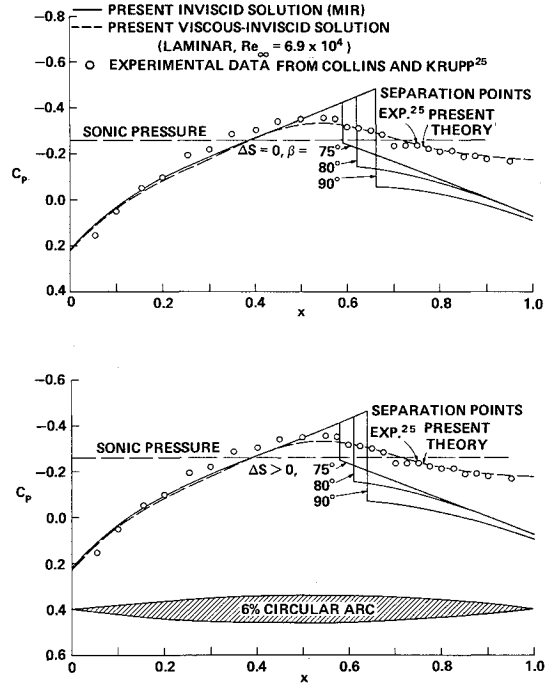

Fig. 8 Pressure distribution over a 6% circular arc at $M_\infty = 0.868$ and $\alpha = 0°$.

the embedded supersonic region although the viscous-inviscid interaction has been strong since $x = 0.37$. The separation point is found when $a = 0$ which corresponds to zero shearing stress at the wall.

The boundary layer keeps separated over the rear of the air-

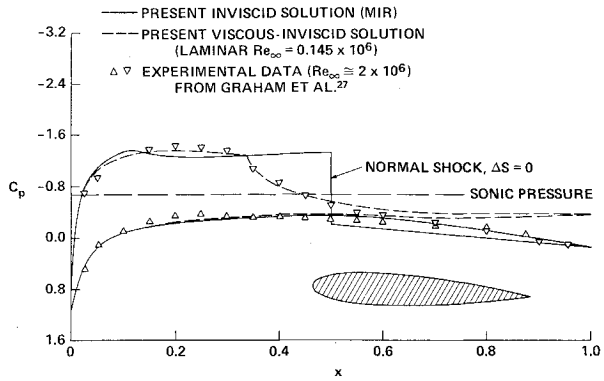

Fig. 9 Pressure distribution on an NACA 0015 airfoil at $M_\infty = 0.729$ and $\alpha = 4°$.

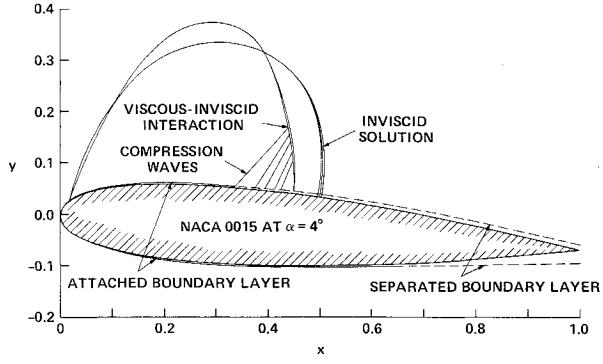

Fig. 10 Flowfield of a NACA 0015 airfoil at $M_\infty = 0.729$, $\alpha = 4°$, and $Re_\infty = 0.145 \times 10^6$.

foil where small adverse pressure gradients are generated by continuous compression of the outer subsonic flow. This is a physical feature of the transonic viscous-inviscid interaction since by compression, the flow ought to return almost to the freestream value downstream. After leaving the trailing edge, the viscous wake contains a reversed flow for a distance and then turns to forward flow downstream. The location of the rear stagnation point agrees well with that found by Klineberg and Steger[9] under similar flow conditions.

As mentioned previously in Iteration III, the flow tends to bracket rather than asymptotically approach the freestream value far downstream. The distribution of variables δ^*, H, and a in Figs. 6 and 7, respectively, give representative mean values after $x = 1.5$. Analytical results for the 6% circular arc airfoil compare very well with recent laminar experimental data of Collins and Krupp[25] as presented in Fig. 8, not only in pressure distribution but also in the separation point. The small difference in freestream Mach number between theory and experiment was deliberately selected to offset wind-tunnel interference effects.[26] Figure 8 also shows the inviscid isentropic and nonisentropic solutions obtained by using the method of integral relations with three different shock conditions. Note that the shock foot is smeared as a result of the strong viscous-inviscid interaction. The inviscid result with $\Delta S > 0$ and $\beta = 75°$ simulates the flow best in the region near the shock; however, it still deviates from the viscous data in the trailing edge. The difference is obviously attributable to the thickening of the laminar boundary layer toward the trailing edge.

On the other hand, comparisons between theory and experiment for the NACA 0015 airfoil were jeopardized because of lack of available laminar test data. Measurements available for this case were taken from Graham et al.[27] at Reynolds numbers on the order of 2×10^6; the flows were, therefore, turbulent. The calculated laminar result is in good agreement with the experimental data in the forward portion of the airfoil; however, there is considerable discrepancy in pressure near the trailing edge; see Fig. 9. The discrepancy may be attributed to the extended separation of the laminar boundary layer, which would be unlikely to occur if the boundary layer were turbulent. Since the method of utilizing reversed-flow velocity profile was originally attempted for application to cases with small adverse pressure gradients,[28] this discrepancy also raised questions regarding the validity of its use in separated boundary layers with strong adverse pressure gradients.

Finally, Fig. 10 shows the overall flowfield of the NACA 0015 airfoil at $M_\infty = 0.729$, $\alpha = 4°$, and $Re_\infty = 0.145 \times 10^6$, based on the chord length. The calculated boundary layer is fairly thin because of the high Reynolds number used. The separated boundary layer on the lower side is thicker than that on the upper side because the latter is developed from a very thin attached layer in an accelerating external flow prior to the shock wave. In any case, the basic features of the transonic viscous-inviscid interaction are clearly seen. The compression waves in the region near the shock are represented by the Mach lines. Being normal to the edge of the boundary layer, the Mach one line represents the end of a smearing shock toe rather than the whole shock. The mechanism of the compression has been designated in the literature as the "lambda shock," which serves as part of the decelerating process of the flow over the rear of the airfoil, where the laminar boundary layer does not have sufficient energy for reattachment against continuous adverse pressure gradients and, therefore, remains separated all the way to the trailing edge.

It is also interesting to note that the viscous-inviscid interaction process terminates the embedded supersonic flow earlier than does the inviscid shock. The result is not surprising since the interaction process has weakened the strength of the shock wave; in turn, it moves the shock forward.[11,12,29] However, because of change of local velocity distribution, the height of the supersonic pocket determined by the present analysis is slightly higher than that obtained by the inviscid solution. The present result of the height of the supersonic pocket remains to be verified by appropriate experiment or other valid analysis.

Conclusions

The boundary-layer integral method coupled with the inviscid method of integral relations provides a relatively simple and adequate means for analyzing the essential features of transonic laminar viscous-inviscid interaction over airfoils. The advantage of the integral relationship in both inviscid and viscous flows is that it allows the flow properties to be computed simultaneously for direct coupling of two flows in strong interaction regions. A limited comparison of the present results for surface pressure, as well as separation point, with recent laminar experimental data yields good agreement.

For supercritical flows, a strong interaction usually occurs, regardless of whether the laminar boundary layer is attached or separated. The boundary layer will eventually become separated even though it is still attached at the shock. In the transonic case (unlike the supersonic), once the laminar boundary layer is separated, it remains separated downstream of the shock. The upper portion of the shock wave retains a finite strength in the external inviscid flow, whereas the shock foot is smeared in the strong viscous-inviscid interaction. The interaction process terminates the embedded supersonic flow earlier than does the inviscid shock. In case of subcritical flows, on the other hand, a weak interaction is usually involved, even if the boundary layer has been separated.

References

[1] Holder, D.W., "The Transonic Flow Past Two-Dimensional Aerofoils," *Journal of the Royal Aeronautical Society,* Vol. 68, Aug. 1964, pp. 501-516.

[2] Sichel, M., "Theory of Viscous Transonic Flow—A Survey," "Transonic Aerodynamics," AGARD CP 35, Sept. 1968.

[3] Pearcey, H.H. and Osborne, J., "Some Problems and Features of Transonic Aerodynamics," ICAS Paper 70-14, Sept. 1970, 7th Congress of the International Council of the Aeronautical Sciences, Rome, Italy.

[4] Liepmann, H.W., "Interaction between Boundary Layers and Shock Waves in Transonic Flow," *Journal of the Aeronautical Sciences,* Vol. 13, Dec. 1946, pp. 223-237.

[5] Ackeret, J., Feldmann, F., and Rott, N., "Investigations of Compression Shocks and Boundary Layers in Gases Moving at High Speeds," TM 1113, Jan. 1947, NACA.

[6] Lighthill, M.J., "On Boundary Layers and Upstream Influence: II. Supersonic Flow with Separation," *Proceedings of the Royal Society: Ser. A: Mathematical and Physical Sciences,* Vol. 217, May 1953, pp. 478-507.

[7] Lees, L. and Reeves, B.L., "Supersonic Separated and Reattached Laminar Flows: I. General Theory and Application of Adiabatic Boundary Layer Shock Wave Interactions," *AIAA Journal,* Vol. 2, Nov. 1964, pp. 1907-1920.

[8] Klineberg, J.M. and Lees, L., "Theory of Laminar Viscous-Inviscid Interactions in Supersonic Flow," *AIAA Journal,* Vol. 17, Dec. 1969, pp. 2211-2221.

[9] Klineberg, J.M. and Steger, J.L., "Calculation of Separated Flows at Subsonic and Transonic Speeds," July 1972, Proceedings of the 3rd International Conference on Numerical Methods in Fluid Mechanics, Vol. II, Springer-Verlag Berlin, 1973, pp. 161-168.

[10] Brilliant, H.M. and Adamson, T.C., Jr., "Shock-Wave-Boundary Layer Interactions in Laminar Transonic Flow," *AIAA Journal,* Vol. 12, March 1974, pp. 323-329.

[11] Tai, T.C., "Application of the Method of Integral Relations to Transonic Airfoil Problems: Part I—Inviscid Supercritical Flow over Symmetric Airfoil at Zero Angle of Attack," Rept. 3424, Sept. 1970; "Part II—Inviscid Supercritical Flow about Lifting Airfoils with Embedded Shock Wave," Rept. 3424-II, July 1972, Naval Ship Research and Development Center, Bethesda, Md.

[12] Tai, T.C., "Transonic Inviscid Flow over Lifting Airfoils by the Method of Integral Relations," *AIAA Journal,* Vol. 12, June 1974, pp. 798-804.

[13] Holder, D.W., Pearcey, H.H., and Gadd, G.W., "The Interaction between Shock Waves and Boundary Layers," CP 180, Feb. 1954, Aeronautical Research Council, London, England.

[14] Oswatitsch, K., "Die Ablösungsbedingung von Grenzschichten," *Symposium on Boundary Layer Research,* edited by H. Görtler, Springer-Verlag Berlin, 1958, pp. 357-367.

[15] Chapman, D.R., Kuehn, D.M., and Larson, H.K., "Investigation of Separated Flows in Supersonic and Subsonic Streams with Emphasis on the Effect of Transition," Rept. 1356, 1958, NACA.

[16] Pearcey, H.H., Osborne, J., and Haines, A.B., "The Interaction between Local Effects at the Shock and Rear Separation—a Source of Significant Scale Effects in Wind-Tunnel Tests on Aerofoils and Wings," AGARD CP 35, Sept. 1968.

[17] Tai, T.C., "Transonic Laminar Visocus-Inviscid Interaction over Airfoils," Report 4362, June 1974, Naval Ship Research and Development Center, Bethesda, Md.

[18] Stewartson, K., "Correlated Incompressible and Compressible Boundary Layers," *Proceedings of the Royal Society: Ser. A: Mathematical and Physical Sciences,* Vol. 200, 1949, pp. 85-100.

[19] Tani, I., "On the Approximate Solution of the Laminar Boundary Layer Equations," *Journal of the Aeronautical Sciences,* Vol. 21, July 1954, pp. 487-495.

[20] Stewartson, K., "Further Solutions of the Falkner-Skan Equation," *Proceedings of the Cambridge Philosophical Society,* Vol. 50, 1954, pp. 454-465.

[21] Klineberg, J.M., Kubota, T., and Lees, L., "Theory of Exhaust-Plume/Boundary-Layer Interactions at Supersonic Speeds," *AIAA Journal,* Vol. 10, May 1972, pp. 581-588.

[22] Kuethe, A.M. and Schetzer, J.D., *Foundations of Aerodynamics,* Wiley, New York, 1959, pp. 72-78.

[23] Pearcey, H.H., "The Aerodynamic Design of Section Shapes for Swept Wings," *Advances in Aeronautical Sciences,* Vol. 3, Pergamon Press, New York, 1961, pp. 227-322.

[24] Schubauer, G.B., "Air Flow in a Separating Laminar Boundary Layer," Rept. 527, 1935, NACA.

[25] Collins, D.J. and Krupp, J.A., "Experimental and Theoretical Investigations in Two-Dimensional Transonic Flow," *AIAA Journal,* Vol. 12, June 1974, pp. 771-778.

[26] Murman, E.M., "Computation of Wall Effects in Ventilated Transonic Wind Tunnels, AIAA Paper 72-1007, Palo Alto, Calif., 1972.

[27] Graham, D.J., Nitzberg, G.E., and Olson, R.N., "A Systematic Investigation of Pressure Distribution at High Speeds over Five Presentative NACA Low-Drag and Conventional Aerofoil Sections," Rept. 832, 1945, NACA.

[28] Lees, L. and Reeves, B.L., "Some Remarks on Integral Moment Methods for Laminar Boundary Layers with Application to Separation and Reattachment," Tech. Rept. 1, Dec. 1961, Firestone Flight Sciences Lab., California Institute of Technology, Pasadena, Calif.

[29] Ferrari, C. and Tricomi, F.G., *Transonic Aerodynamics,* translated by R.H. Cramer, Academic Press, New York, 1968, pp. 586-589.